



# An ion-selective separator suppresses polysulfides shuttle for advanced lithium–sulfur batteries

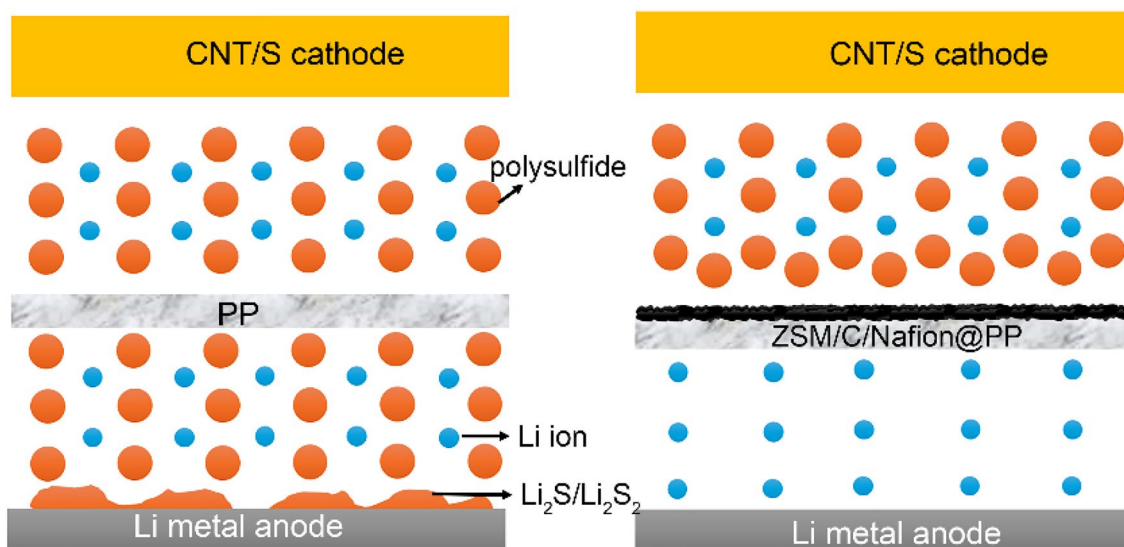
Huajin Mao<sup>1</sup> · Lijuan Yi<sup>2</sup> · Wanning Li<sup>3</sup>

Received: 28 April 2024 / Accepted: 29 June 2024  
© The Author(s), under exclusive licence to Springer Nature B.V. 2024

## Abstract

The lithium–sulfur (Li–S) battery exhibits a high energy capacity that significantly substitutes that of current Li-ion batteries. However, it suffers from severe soluble polysulfide shuttling. Here, we report a zeolite/carbon/Nafion-modified PP (ZSM/C/Nafion@PP) separator to inhibit soluble polysulfide shuttling and improve Li-ion transfer. We demonstrate that the ZSM/C/Nafion@PP separator functions as an ion-selective barrier in Li–S batteries. It facilitates the rapid transport of Li-ions while effectively preventing the migration of polysulfides to the Li metal anode, utilizing a size-exclusion mechanism. As a result, the Li–S battery with the ZSM/C/Nafion@PP separator features a high initial discharge capacity, superior cycling stability (with a low-capacity decay rate of 0.059% per cycle over 600 cycles at 1 C), and rate performance (954 mA g<sup>-1</sup> at 2 °C). Moreover, the Li–S battery with a high S loading cathode (5.6 mg cm<sup>-2</sup>) and low E/S ratio (6.3 μL mg<sup>-1</sup>) displays a high initial discharge capacity of 966 mA g<sup>-1</sup> and superior cycling stability over 200 cycles at 0.5 °C. This work shows the potential for ZSM-based materials as functional coatings for highly stable Li–S batteries.

## Graphical abstract



**Keywords** Lithium–sulfur batteries · Polysulfide shuttling · ZSM · Separator · Cycling stability

Extended author information available on the last page of the article

Published online: 09 July 2024

## 1 Introduction

Lithium-ion batteries are widely used in portable electronic devices, mobile communications, electric vehicles, and other fields [1–3]. However, with the escalating demand for high energy-density storage devices, existing lithium-ion batteries are no longer able to satisfy this need. Lithium–sulfur (Li–S) batteries, as the most promising next-generation battery energy storage technology, have the potential to break through the energy density bottleneck of lithium-ion batteries and have attracted much attention in recent years [4, 5]. However, the shuttling of soluble polysulfide ( $\text{Li}_2\text{S}_x$ ,  $4 \leq x \leq 8$ ) in Li–S batteries will lead to serious decreases in capacity, cycle stability, and Coulombic efficiency [6, 7].

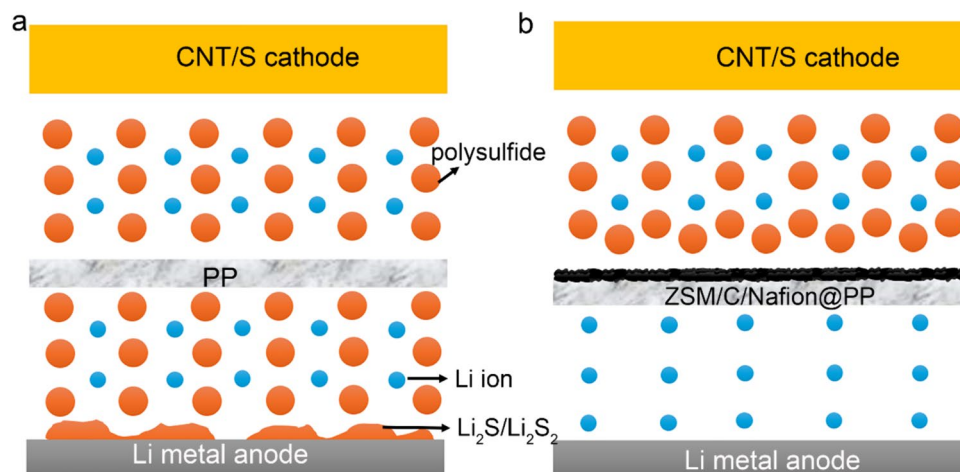
Recent studies have shown that polymer separators are not only crucial to the safety of batteries [8, 9], but also can effectively inhibit the shuttle of intermediate products, regulate the growth of dendrites on the surface of metal anodes, improve ion transfer, and improve the stability of electrode interfaces in Li metal batteries [7, 10]. Polyolefin separators (PE, PP, etc.) have many excellent properties and are widely used in lithium-ion batteries [2, 11]. However, polyolefin separators have large and non-uniform pore sizes with hundreds of nanometers. Therefore, polysulfides can freely pass through the polyolefin separator and deposit on the Li metal anode surface (Fig. 1a) [12]. This will not only lead to passivation of the lithium metal anode and loss of active materials, but also seriously reduce the cycle stability of Li–S batteries [13, 14]. Surface functionalization of polyolefin separators is one of the effective ways to solve the problem of polysulfide shuttle and improve the comprehensive performance of Li–S batteries [15–17].

Various carbon materials have been used to modify the polyolefin separators [18–21]. However, non-polar

carbon materials have only weak physical adsorption on polar polysulfides and cannot maintain the long-term cycle stability of Li–S batteries [22]. Therefore, some polar materials are used to modify the polyolefin separators to inhibit polysulfide shuttle through chemical adsorption and physical adsorption, such as functionalized carbon materials [23–25], metal compounds [26–29], organic polymers [30–32], clay minerals [33–35], and so on. These functionalized separators can effectively inhibit polysulfide shuttles, thereby improving the electrochemical performance of Li–S batteries [36, 37].

Zeolites are a type of aluminosilicate with uniform micropores, mainly composed of silicon, aluminum, oxygen and other metal cations [38]. With ion exchange, adsorption, catalysis, stability, chemical reactivity, and zeolites have been widely used in the petrochemical industry, environmental protection, bioengineering, food industry, pharmaceutical chemical industry, energy storage, and other fields [38]. Recently, a few studies demonstrated that zeolites are very potential materials in energy storage applications, including multifunctional additives for cathode [39] and active fillers for solid electrolytes [40, 41]. And then, Wu et al. [42] prepared a composite polymer electrolyte based on lithiated X type zeolite for advanced Li batteries. The composite polymer electrolyte displays a high ionic conductivity of  $1.98 \times 10^{-4}$  S/cm, high  $\text{Li}^+$  transference number of 0.55, a wide electrochemical window of 4.7 V, and excellent stability toward Li metal anode [42]. In Yu and Xu group, [43] reported a lithium-ion-exchanged zeolite inorganic solid electrolyte membrane for high-performance Li-air battery. The Li-air battery shows a high capacity of  $12,020 \text{ mAh g}^{-1}$  and a good cycle life of 149 cycles at a current density of  $500 \text{ mA g}^{-1}$ . Zeolites have uniform pore sizes, which may be used for efficiently inhibiting polysulfides in Li–S batteries. To the best of our knowledge, there has been no report about zeolites modifying polyolefin separators to date in highly stable Li–S batteries.

**Fig. 1** Schematic illustrations of the Li–S batteries with the **a** PP and **b** ZSM/C/Nafion@PP separators



In this work, we report a ZSM/C/Nafion@PP separator designed specifically for the highly stable Li–S battery, functioning as an ion-selective separator to selectively pass through Li-ions while inhibiting polysulfide shuttling (Fig. 1b). We chose zeolite socony mobil-35 (ZSM-35) as a coating material for the preparation of the ZSM/C/Nafion@PP separator because of its two-dimensional channel structure with a size range of approximately  $5.4 \times 4.2 \text{ \AA}$ , which is significantly smaller than the size of polysulfides ( $\text{Li}_2\text{S}_x$ ,  $4 < x \leq 8$ ). Therefore, it may be effectively utilized to inhibit polysulfides and improve Li-ion transport in Li–S batteries through the size effect. The ZSM/C/Nafion@PP separator displayed high efficiency in inhibiting polysulfide shuttle and superior cycling stability in a Li–S battery. The battery possesses low capacity-fading rates of 0.059% per cycle over 600 cycles at 1 °C and good rate performance. Moreover, the Li–S battery with a high S loading cathode ( $5.6 \text{ mg cm}^{-2}$ ) and low E/S ratio ( $6.3 \text{ \mu L mg}^{-1}$ ) displays a high initial discharge capacity and superior cycling stability over 200 cycles at 0.5 °C.

## 2 Experimental section

### 2.1 Materials and characteristics

ZSM-35 was acquired from Zhuoyue Environmental Protection New Materials (Shanghai) Co., Ltd. Super P, PVDF, CNTs, PP separator, electrolyte, S powder, 1-methyl-2-pyrrolidinone (NMP), isopropanol, and  $\text{Li}_2\text{S}$  were purchased from Guangdong Canrd New Energy Technology Co., Ltd., China. All chemical reagents were utilized as received without necessitating further purification.

Transmission electron microscopy (TEM) images were captured using a TECNAI G2F20. Scanning electron microscopy (SEM) was conducted with a JSM6700F field-emission scan electron microscope. Raman spectra were obtained through confocal microprobe Raman spectroscopy, utilizing the LabRAM HR Evolution from HORIBA Jobin Yvon.

### 2.2 Preparation of ZSM/C/Nafion@PP separator

ZSM-35 and carbon material (Super P) are dispersed into isopropanol, stirred for 2 h, followed by sonication for 1 h to obtain a uniform suspension as A. Subsequently, a solution containing 2% Nafion is added to suspension A, and it is then stirred for 6 h to obtain suspension B. Then, the suspension B is deposited on one side of the PP surface via vacuum filtration. The ion-selective membrane (ZSM/C/Nafion@PP) is obtained after being placed under vacuum conditions at 60 °C for 12 h. The carbon material-coated PP (C@PP) is prepared by the same method. The coating load is  $0.78 \text{ mg cm}^2$ .

### 2.3 Preparation of CNT/S cathodes

The S cathode was prepared using a simple doctor-blade coating technique. Typically, the mixture of 80% CNT/S, 15 wt% super P, and 5 wt% PVDF was combined with NMP to create a slurry. This slurry was subsequently cast onto carbon-coated Al foil and allowed to dry at a temperature of 60 °C for a duration of 12 h. The CNT/S was prepared by the traditional heat treatment method. Typically, S powder and CNTs were ground together in an appropriate mass ratio. The resultant mixture was then heated at a temperature of 155 °C for a period of 12 h.

### 2.4 Battery assembly and testing

The CR2032 coin-type cells were used to evaluate the effect of the separator on the performance of Li–S batteries. The batteries were assembled in an argon-filled glovebox, utilizing Li metal as the anode, CNT/S cathodes, and separators (PP, C@PP, or ZSM/C/Nafion@PP). 1 M lithium bis(trifluoromethane) sulfonimide with 2%  $\text{LiNO}_3$  dissolved in a mixture of 1,3-dioxolane and dimethoxymethane (DOL/DME, 1:1 by volume) was used as an electrolyte. The S loadings of the CNT/S cathodes are  $1.3 \text{ mg cm}^{-2}$  and  $5.6 \text{ mg cm}^{-2}$ , respectively. The electrolyte/sulfur (E/S) ratio was  $11 \text{ \mu L mg}^{-1}$  for  $1.3 \text{ mg cm}^{-2}$  and  $6.3 \text{ \mu L mg}^{-1}$  for  $5.6 \text{ mg cm}^{-2}$ . Electrochemical performances were examined within a voltage range of 1.6 to 2.8 V using a Neware battery test system provided by Neware Technology Co. Cyclic voltammetry (CV) curves were generated at a rate of  $0.2 \text{ mV s}^{-1}$  on a CHI604E electrochemical workstation.

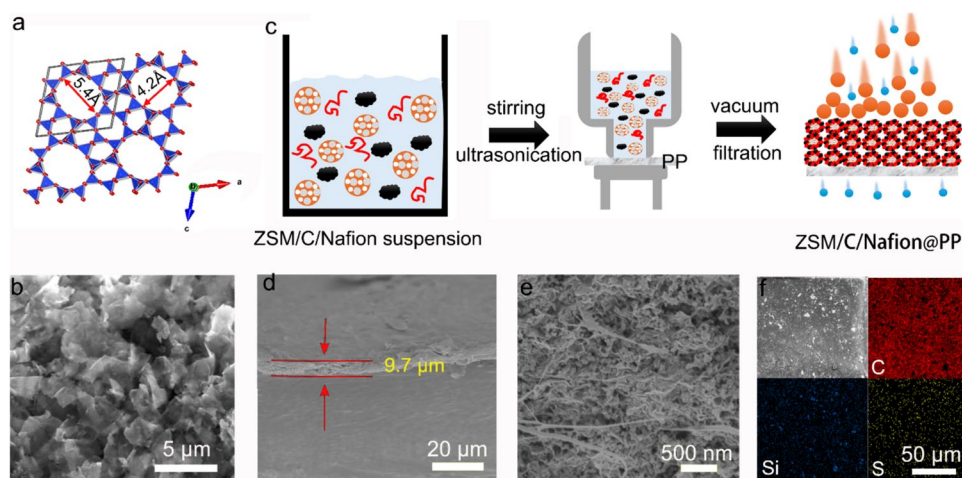
### 2.5 Permeation test of polysulfides

Polysulfide ( $\text{Li}_2\text{S}_6$ ) was synthesized through a chemical reaction between sulfur (S) and  $\text{Li}_2\text{S}$  in a DOL/DME (v:v = 1:1) solution, maintaining a molar ratio of 5:1. The mixed solution was stirred in an argon-filled glovebox at 60 °C for 48 h to produce a brownish-red polysulfide solution. A permeation test was subsequently conducted using an H-type cell, which was separated by separators. In this setup, the left tube contained 20 mL of the polysulfide solution (0.2 M, primarily composed of  $\text{Li}_2\text{S}_6$ ), while the right tube held 20 mL of DOL/DEM.

## 3 Results and discussion

ZSM-35 molecular sieve ( $\text{Mg}^{2+}\text{Na}^+(\text{H}_2\text{O})_{18}[\text{Al}_6\text{Si}_{30}\text{O}_{72}]$ ), also known as ferrierite, belongs to the orthorhombic crystal system with FER-type topology. It possesses a typical 2D pore channel structure (Fig. 2a), which is formed by the vertical intersection of eight-membered and ten-membered rings. The ZSM-35 shows a nanosheet structure and highly ordered nanopores (Fig. 2b), with a size range of

**Fig. 2** **a** An illustration of the microporous crystalline structures and **b** TEM images of the SEM-35. **c** Schematic diagram of the preparation of the ZSM/C/Nafion@PP separator. **d** Surface and **e** cross-sectional SEM images, and **f** EDS mapping of the ZSM/C/Nafion@PP separator



approximately  $5.4 \times 4.2 \text{ \AA}$ , which is significantly smaller than the size of polysulfides ( $> 13 \text{ \AA}$ ) [44, 45]. Therefore, the ZSM-35 may be effectively utilized to inhibit polysulfides and improve Li-ion transport in Li-S batteries through the size effect.

To verify the inhibition ability of ZSM-35 on polysulfide, a ZSM-35 composite-modified PP separator was prepared through vacuum filtration. The preparation procedure is shown in Fig. 2c. The ZSM/C/Nafion@PP separators were prepared by deposition of a suspension containing ZSM-35, carbon material, and Nafion onto one side of the PP separator surface. The ZSM/C/Nafion coating layer on the PP separator is  $0.78 \text{ mg cm}^{-2}$ . The PP separator shows a highly porous matrix with a pore size of several hundreds of nanometers, which allows the free shuttle of polysulfide. After coating, it is covered by the ZSM/C/Nafion coating layer (Fig. 2d). Based on the cross-sectional SEM image of the ZSM/C/Nafion@PP separator (Fig. 2e), the thickness of the ZSM/C/Nafion coating layer on the PP separator surface is about  $9.7 \text{ \mu m}$ . It can be seen from Fig. 2f that the homogeneous distribution of the ZSM-35 nanorods in the ZSM/C/Nafion coating layer is confirmed by the strong and uniform Si map that originated from ZSM-35. The strong and uniform S and C maps also demonstrate a homogeneous distribution of carbon material and Nafion on the whole surface of the ZSM/C/Nafion coating layer.

The ZSM/C/Nafion@PP separator exhibits commendable flexibility, capable of being repeatedly folded numerous times without exfoliation (Fig. 3a). Furthermore, the ZSM/C/Nafion@PP separator demonstrates a significantly lower contact angle for the electrolyte (approximately  $0^\circ$ ) due to its hydrophilicity, which is markedly superior to those observed on PP ( $45^\circ$ ) (Fig. 3b). This suggests that the ZSM/C/Nafion@PP separator possesses enhanced wettability and affinity toward the electrolyte.

Fast Li-ion transfer is critical to obtain excellent electrochemical performance. However, traditional coated

separators usually show a low ionic conductivity, mainly because the coating layer not only increases the interfacial resistance of the battery but also blocks the transfer channel of Li-ions [6, 46]. According to EIS measurements (Fig. 3c), the ZSM/C/Nafion@PP separator displays a high ionic conductivity of  $1.43 \times 10^{-3} \text{ S cm}^{-1}$ , which is significantly superior to that of PP ( $0.63 \times 10^{-3} \text{ S cm}^{-1}$ ) and C@PP ( $0.67 \times 10^{-3} \text{ S cm}^{-1}$ ) separators. Interestingly, Li-ion transfer number of the ZSM/C/Nafion@PP separator (0.62) is also higher than those of the PP (0.35) C@PP (0.37) separators (Figs. 3d–g and S1). This is due to the ZSM-35 nanosheets that facilitate Li-ion diffusion. In addition, the superior electrolyte wettability of the ZSM/C/Nafion@PP separator also contributes to the fast Li-ion transfer.

As a superior separator, the inhibition capability to polysulfide shuttle in a Li-S battery is an important factor, which is often evaluated using a polysulfide permeation testing in H-shaped glass bottles. Typically, the polysulfide (mainly  $\text{Li}_2\text{S}_6$ ) solution was slowly added into the left-side glass bottles. Then, a blank DOL/DEM solution was slowly added into the right-side glass bottle. The polysulfide permeation with the PP separator was tested under similar conditions.

In the H-shaped glass bottle with the PP separator (Fig. 4a), almost 1/2th of the right-side glass bottle was filled with a yellow polysulfide solution within a span of 12 h. However, polysulfides underwent an accelerated pass through the PP separator and entered the right-side glass bottle until polysulfide completely occupied the blank electrolytes within 24 h. Meanwhile, in the H-shaped glass bottle with the C@PP separator (Fig. 4b), 1/3th of the right-side glass bottle was filled with a yellow polysulfide solution within a span of 12 h. After 24 h, the almost 1/2th of the right-side glass bottle was filled with a yellow polysulfide solution. In contrast, no obvious change could be observed after 24 h for the H-shaped glass bottle with the ZSM/C/Nafion@PP separator (Fig. 4b), demonstrating its strong capability to inhibit the polysulfide shuttling.



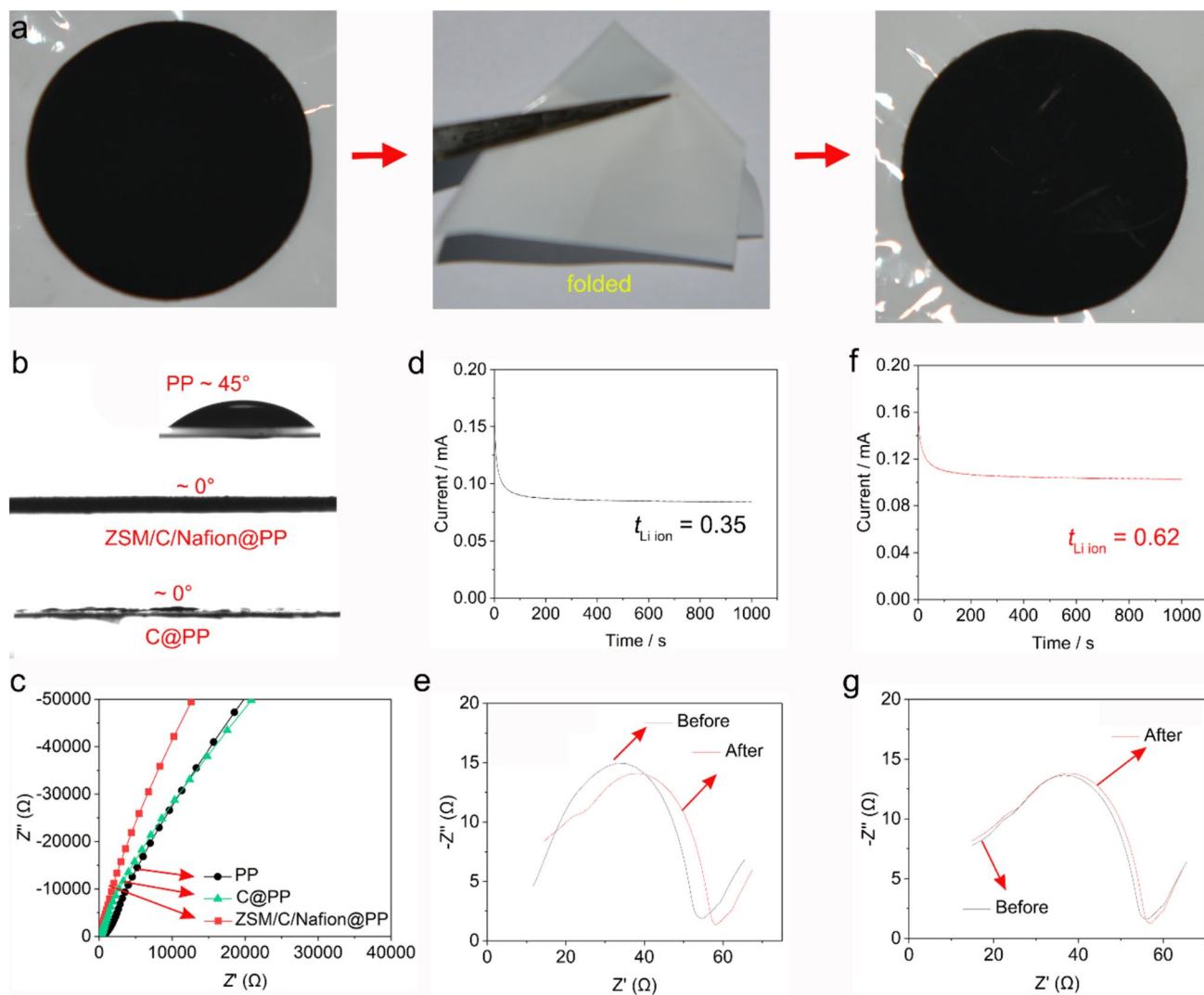


**Fig. 3** **a** Photographs of the ZSM/C/Nafion@PP separator. **b** Contact angles of the electrolyte on the surface of the separator. **c** Nyquist plots of ionic conductivity. Current variations with time during polar-

ization and Nyquist plots of the cells assembled using the **d, e** PP and **f, g** ZSM/C/Nafion@PP separators

To evaluate the performance of the ZSM/C/Nafion@PP separator in Li–S batteries, it was assembled with the CNT/S cathode into CR2032 coin cells within an argon-filled glove box. The ZSM/C/Nafion coating layer faced the CNT/S cathode (Fig. 1b). Figure 5a shows the CV curves of the Li–S batteries with different separators. All of the batteries show three peaks. On the anodic scan, one strong oxidation peak at 2.5 V is observed, which is due to the oxidization of  $\text{Li}_2\text{S}/\text{Li}_2\text{S}_2$  to  $\text{S}_8$  [47, 48]. On the cathodic scan, the two reduction peaks were observed at 2.01 and 2.28 V, respectively, which correspond to the reduction of  $\text{S}_8$  to soluble  $\text{S}_x^{2-}$  and the reduction of  $\text{S}_x^{2-}$  to  $\text{Li}_2\text{S}/\text{Li}_2\text{S}_2$ . [49, 50] Obviously, the Li–S battery with the ZSM/C/Nafion@PP separator displays a higher oxidation peak and reduction peak, which is higher than that of the C@PP and PP separators. These

results demonstrate that the ZSM/C/Nafion@PP separator can effectively improve the electrochemical performance of Li–S batteries.

The Li–S battery with the ZSM/C/Nafion@PP separator was tested at 1 °C ( $1\text{ °C} = 1670\text{ mA g}^{-1}$ ) over 600 cycles (Fig. 5b). The high initial discharge capacity of  $909\text{ mA h g}^{-1}$  was obtained, followed by a drop up to the 40th cycle. The decay of capacity is due to the activation cycles leading to a highly reversible and stable electrochemical status [44, 46]. The discharge capacity still approached  $634\text{ mA g}^{-1}$ ,  $646\text{ mA g}^{-1}$ ,  $620\text{ mA g}^{-1}$ ,  $597\text{ mA g}^{-1}$ ,  $579\text{ mA g}^{-1}$ , and  $588\text{ mA g}^{-1}$  at the end of the 100th, 200th, 300th, 400th, 500th, and 600th cycles, respectively. These results suggest that the Li–S battery with the ZSM/C/Nafion@PP separator shows good reversibility and cycling stability, with a low

**Fig. 4** Polysulfide permeation measurements: **a** PP, **b** C@PP and **c** ZSM/C/Nafion@PP separator, showing polysulfide diffusion from the left side to the right side in the H-shaped glass bottles

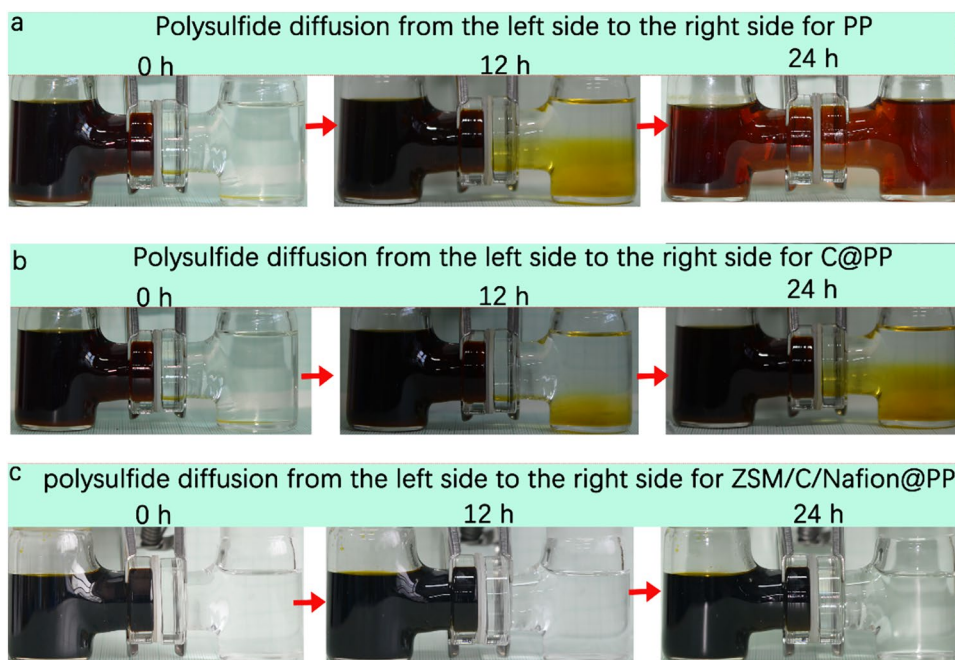
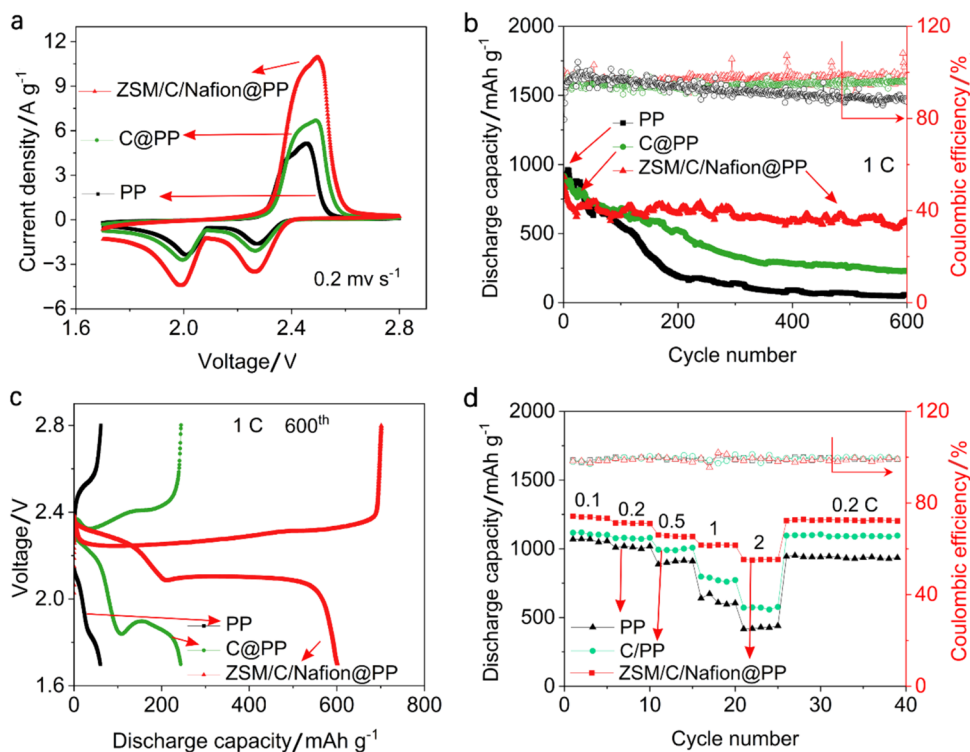


**Fig. 5** Electrochemical performances of Li–S batteries with different separators. **a** CV curves at  $0.2 \text{ mV S}^{-1}$ . **b** Cycle stability and Coulombic efficiency at a rate of 1 C. **c** Charge–discharge profiles at the 600th cycle at a rate of 1 C. **d** Rate performance comparison at varying current densities



fade rate of 0.059% per cycle and a high Coulombic efficiency of 98.7%, superior to those with the C@PP separator (0.13% and 95.78%) and PP separator (0.17% and 91.6%). Notably, the discharge–charge curve of the Li–S battery with the ZSM/C/Nafion@PP separator shows one long oxidation plateau and two reduction plateaus after 600 cycles (Fig. 5c), which is consistent with the CV curves. Moreover, the Li–S

battery with the ZSM/C/Nafion@PP separator has the lowest voltage hysteresis, showing low resistance and rapid electrochemical redox reactions. However, no obvious discharge plateau can be seen in the Li–S battery with the PP separator. This is because the ZSM/C/Nafion@PP separator can effectively inhibit polysulfide shuttling and then maintain cycling stability.

To better understand the redox behavior, Li–S batteries with different separators were tested at different rates (Fig. 5d). The Li–S battery with the ZSM/C/Nafion@PP separator features a good rate capacity that can be maintained at different rates. When cycling at 0.1, 0.2, 0.5, 1, and 2 °C, the discharge capacities were maintained at 1236 mA g<sup>-1</sup>, 1196 mA g<sup>-1</sup>, 1095 mA g<sup>-1</sup>, 1015 mA g<sup>-1</sup>, and 954 mA g<sup>-1</sup>, respectively. Significantly, rate capacities recover to 1218 mA h g<sup>-1</sup> when the rate switches back to 0.2 °C, indicating that the ZSM/C/Nafion@PP separator has good stability and reversibility in Li–S battery. However, the Li–S batteries with the PP and C@PP separator show a dramatic discharge capacity decay from 0.5 to 1 °C. The initial discharge capacity at 0.1 °C can reach up to 1121 mA g<sup>-1</sup> and 1067 mA g<sup>-1</sup>, respectively, decreasing to final value of 567 mA g<sup>-1</sup> and 409 mA g<sup>-1</sup>, respectively. Obviously, the Li–S battery with the ZSM/C/Nafion@PP separator has the highest capacity retention rate of 77.18% from 0.1 to 2 °C compared to the PP separator (38.33%) and C@PP separator (50.58%).

It is well known that the polysulfide shuttle will lead to the deposition of Li<sub>2</sub>S/Li<sub>2</sub>S<sub>2</sub> on surface of the Li metal anode, causing Li anode degradation [51, 52]. Therefore, the morphology and chemical composition of the cycled Li metal anode were analyzed to evaluate the separator's capability to inhibit polysulfides. Figure 6a shows SEM images of the cycled Li metal anodes in Li–S battery with the PP

separator. Enriched irregular holes and cracks on the surface of cycled Li metal anode show that the Li metal anode is severely corroded by polysulfides with the PP separator after cycles. However, the cycled Li metal anode surface in Li–S battery with the ZSM/C/Nafion@PP separator shows a relatively ideal morphology with fewer holes and no flaky dendrites (Fig. 6b). This shows that the ZSM/C/Nafion@PP separator can effectively prevent the deterioration of the Li metal anode structure. Raman spectroscopy is performed to analyze the chemical composition of the cycled Li metal anode surface. As shown in Fig. 6c, polysulfide species shuttle pass through the PP separator and form Li<sub>2</sub>S, Li<sub>2</sub>S<sub>2</sub>, Li<sub>2</sub>S<sub>4</sub>, Li<sub>2</sub>S<sub>6</sub>, and Li<sub>2</sub>S<sub>8</sub>, which shows that the PP separator cannot inhibit the shuttle of polysulfide. In contrast, weaker polysulfide signals are observed on the cycled Li metal anode surface with the ZSM/C/Nafion@PP separator (Fig. 6d), showing the effectively eliminated shuttling of polysulfides due to the strong size effect.

To demonstrate the advantages of the ZSM/C/Nafion@PP separator in practical Li–S battery, the cycling performance of the Li–S batteries with high S loading (5.6 mg cm<sup>-2</sup>) and low E/S ratio (6.3 μL mg<sup>-1</sup>) was also evaluated at 0.5 °C. Although both batteries exhibit one charge plateau and two discharge plateaus (Fig. 7a), the Li–S battery with ZSM/C/Nafion@PP separator shows a lower voltage hysteresis (0.16 V) and a higher initial discharge capacity (966 mA g<sup>-1</sup>) than that of the PP (0.22 V and 591 mA g<sup>-1</sup>) and C@PP

**Fig. 6** SEM images of the cycled Li metal anode in Li–S batteries with **a** PP and **b** ZSM/C/Nafion@PP separator. Raman spectra of the cycled Li metal anode surface in Li–S batteries with the **c** PP and **d** ZSM/C/Nafion@PP separators

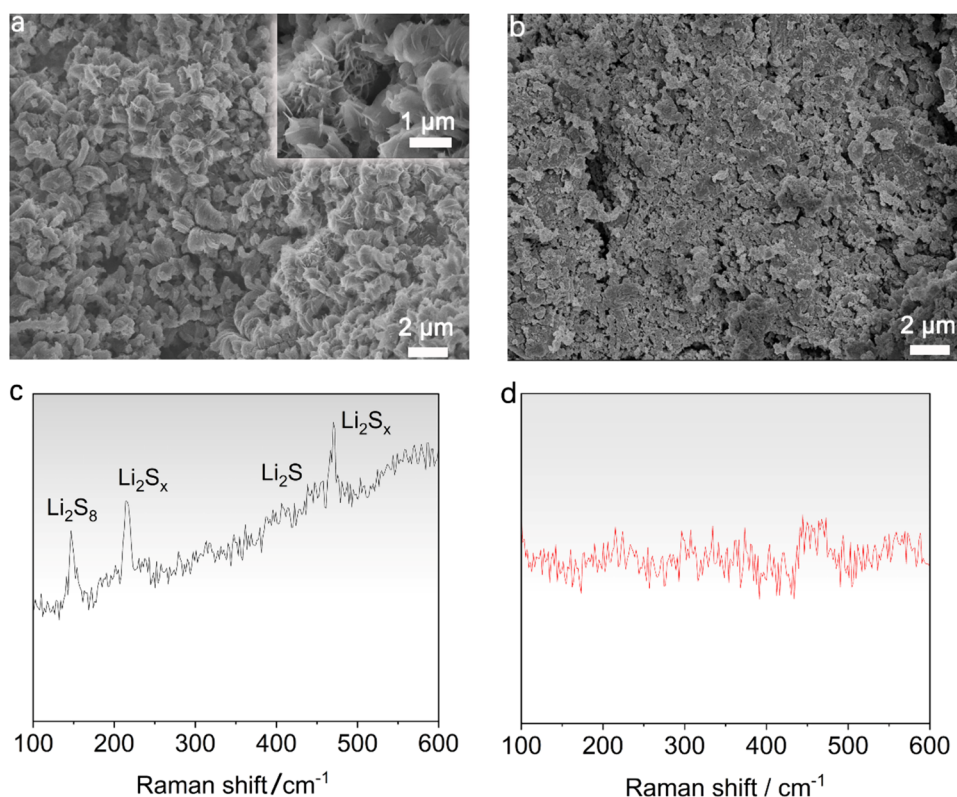
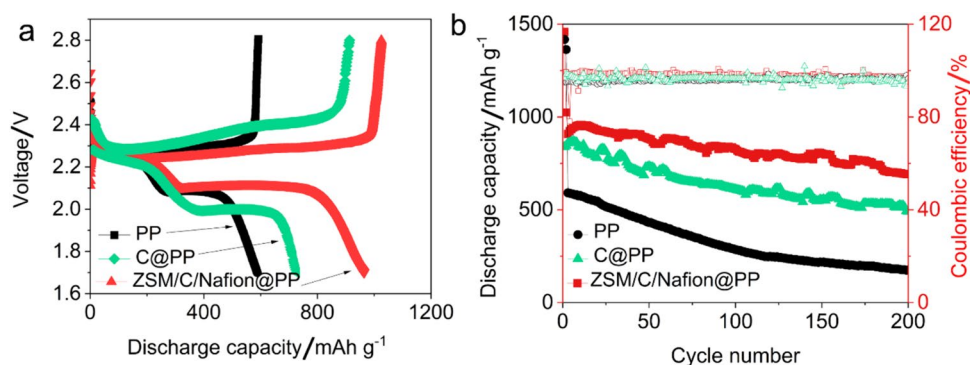




**Fig. 7** **a** Discharge/charge curves at 1st and **b** cycling performance of the Li–S battery with high S loading and low E/S ratio at 0.5 °C



(0.29 V and 791 mA g<sup>-1</sup>) separators. Notably, the Li–S battery with the ZSM/C/Nafion@PP separator exhibits long-term cycling stability at 0.5 °C (Fig. 7b). The initial specific capacity of 966 mA h g<sup>-1</sup> is only decreased to 693 mA h g<sup>-1</sup> after 200 cycles, the average capacity decay per cycle is only 0.14%. However, the Li–S battery with the PP separator exhibits fast capacity decay with a high-capacity decay rate of 0.38% and a low Coulombic efficiency of 95.2%. These results further indicate that high sulfur utilization and excellent cycling stability under a high S loading and a low E/S ratio can be enhanced by the ZSM/C/Nafion@PP separator.

## 4 Conclusion

In summary, we have successfully designed and prepared a ZSM/C/Nafion@PP separator for advanced Li–S batteries. In Li–S batteries, the ZSM/C/Nafion@PP separator can effectively inhibit polysulfide shuttle and improve Li-ion transfer simultaneously. Moreover, the ZSM/C/Nafion@PP separator shows high ionic conductivity and Li-ion transfer number, excellent mechanical stability, and good electrolyte wettability. The Li–S battery with the ZSM/C/Nafion@PP separator displayed sustainably enhanced cycling stability and rate performance. The stable performance is mainly attributed to size effects, which are derived from the homogeneous porous frameworks of the ZSM-35. The strategy demonstrated here sheds a new light on the design and preparation of functional separators based on ZSM for advanced Li–S batteries.

**Supplementary Information** The online version contains supplementary material available at <https://doi.org/10.1007/s10800-024-02165-1>.

**Acknowledgements** This work was supported by the funding from the Datong City Science and Technology Plan Project, Shanxi (2023078463). We thank the helpful testing service from Ceshigo Research Service company.

**Author contributions** Huajin Mao: Conceptualization, Methodology, Supervision, Writing - original draft, and Writing - review & editing.

Lijuan Yi: Conceptualization, Methodology, and Writing - review & editing. Wanning Li: Methodology and Writing - original draft.

## Declarations

**Competing interests** The authors declare no competing financial interests.

## References

- Zeng G, Chen D, Zhen C, Feng C, Pang Y, He W (2023) Amorphous Fe-phytate enables fast polysulfide redox for high-loading lithium sulfur batteries. *Small* 19:2302548
- Yang Y, Wang W, Meng G, Zhang J (2022) Function-directed design of battery separators based on microporous polyolefin membranes. *J Mater Chem A* 10:14137
- Zhang X, Sun Q, Zhen C, Niu Y, Han Y, Zeng G, Chen D, Feng C, Chen N, Lv W, He W (2021) Recent progress in flame-retardant separators for safe lithium-ion batteries. *Energy Storage Mater* 37:628–647
- Hou L-P, Zhang X-Q, Li B-Q, Zhang Q (2021) Challenges and promises of lithium metal anode by soluble polysulfides in practical lithium–sulfur batteries. *Mater Today* 45:62–76
- Zeng G, Liu Y, Chen D, Zhen C, Han Y, He W (2021) Natural lepidolite enables fast polysulfide redox for high-rate lithium sulfur batterie. *Adv Energy Mater* 11:2102058
- Yang Y, Wang W, Li M, Zhou S, Zhang J, Wang A (2023) Plant leaf-inspired separators with hierarchical structure and exquisite fluidic channels for dendrite-free lithium metal batteries. *Small* 19:2301237
- Yang Y, Zhang J (2021) Layered nanocomposite separators enabling dendrite-free lithium metal anodes at ultrahigh current density and cycling capacity. *Energy Storage Mater* 37:135–142
- Yuan N, Sun W, Yang J, Gong X, Liu R (2021) Multifunctional MOF-based separator materials for advanced lithium-sulfur batteries. *Adv Mater Interfaces* 8:2001941
- Zhai P, Liu K, Wang Z, Shi L, Yuan S (2021) Multifunctional separators for high-performance lithium ion batteries. *J Power Sources* 499:229973
- Zhang W, Tu Z, Qian J, Choudhury S, Archer LA, Lu Y (2017) Design principles of functional polymer separators for high-energy, metal-based batteries. *Small* 14:1703001
- Lu W, Yuan Z, Zhao Y, Zhang H, Zhang H, Li X (2017) Porous membranes in secondary battery technologies. *Chem Soc Rev* 46:2199–2236



12. Ren W, Zheng Y, Cui Z, Tao Y, Li B, Wang W (2021) Recent progress of functional separators in dendrite inhibition for lithium metal batteries. *Energy Storage Mater* 35:157–168
13. Hao H, Hutter T, Boyce BL, Watt J, Liu P, Mitlin D (2022) Review of multifunctional separators: stabilizing the cathode and the anode for alkali (Li, Na, and K) metal-sulfur and selenium batteries. *Chem Rev* 122:8053–8125
14. Chen H, Wu Z, Zheng M, Liu T, Yan C, Lu J, Zhang S (2022) Catalytic materials for lithium-sulfur batteries: mechanisms, design strategies and future perspective. *Mater Today* 52:364–388
15. Zhao Q, Wang R, Wen J, Hu X, Li Z, Li M, Pan F, Xu C (2022) Separator engineering toward practical Li-S batteries: Targeted electrocatalytic sulfur conversion, lithium plating regulation, and thermal tolerance. *Nano Energy* 95:106982
16. Li Y, Lin S, Wang D, Gao T, Song J, Zhou P, Xu Z, Yang Z, Xiao N, Guo S (2020) single Atom array mimic on ultrathin MOF nanosheets boosts the safety and life of lithium-sulfur batteries. *Adv Mater* 32:1906722
17. Li Z, Sun Y, Wu X, Yuan H, Yu Y, Tan Y (2022) Boosting adsorption and catalysis of polysulfides by multifunctional separator for lithium-sulfur batteries. *ACS Energy Lett* 7:4190–4197
18. Zhu D, Long T, Xu B, Zhao Y, Hong H, Liu R, Meng F, Liu J (2021) Recent advances in interlayer and separator engineering for lithium-sulfur batteries. *J Energy Chem* 57:41–60
19. Yang B, Wang L, Zhang M, Li W, Zhou Q, Zhong L (2021) Advanced separators based on aramid nanofiber (ANF) membranes for lithium-ion batteries: a review of recent progress. *J Mater Chem A* 9:12923–12946
20. Chen K, Zhang G, Xiao L, Li P, Li W, Xu Q, Xu J (2021) Poly-aniline encapsulated amorphous  $V_2O_5$  nanowire-modified multifunctional separators for lithium-sulfur batteries. *Small Methods* 5:2001056
21. Long X, Luo ZH, Zhou WH, Zhu SK, Song Y, Li H, Geng CN, Shi B, Han ZY, Zhou GM, Lv W, Shao JJ (2022) Two-dimensional montmorillonite-based heterostructure for high-rate and long-life lithium-sulfur batteries. *Energy Storage Materials* 52:120–129
22. Li W, Qin Y, Dou X, Hu Q, Liang W, Nie G, Zhu G, Zeng C, Zeng G (2024) Diminishing self-discharge of high-loading Li-S batteries with oxygen-rich biomass carbon interlayer. *Chem Asian J* 19:e20240017
23. Du Z, Chen X, Hu W, Chuang C, Xie S, Hu A, Yan W, Kong X, Wu X, Ji H, Wan LJ (2019) Cobalt in nitrogen-doped graphene as single-atom catalyst for high-sulfur content lithium-sulfur batteries. *J Am Chem Soc* 141:3977–3985
24. Pei F, Lin L, Fu A, Mo S, Ou D, Fang X, Zheng N (2018) A two-dimensional porous carbon-modified separator for high-energy-density Li-S batteries. *Joule* 2:323–336
25. Balach J, Jaumann T, Klose M, Oswald S, Eckert J, Giebeler L (2015) Functional mesoporous carbon-coated separator for long-life, high-energy lithium-sulfur batteries. *Adv Func Mater* 25:5285–5291
26. Zhang C, Fei B, Yang D, Zhan H, Wang J, Diao J, Li J, Henkelman G, Cai D, Biendicho JJ, Morante JR, Cabot A (2022) Robust lithium-sulfur batteries enabled by highly conductive  $WSe_2$ -based superlattices with tunable interlayer space. *Adv Func Mater* 32:2201322
27. Yao W, Tian C, Yang C, Xu J, Meng Y, Manke I, Chen N, Wu Z, Zhan L, Wang Y, Chen R (2022) P-Doped  $NiTe_2$  with te-vacancies in lithium-sulfur batteries prevents shuttling and promotes polysulfide conversion. *Adv Mater* 34:2106370
28. Song X, Chen G, Wang S, Huang Y, Jiang Z, Ding LX, Wang H (2018) Self-assembled close-packed  $MnO_2$  nanoparticles anchored on a polyethylene separator for lithium-sulfur batteries. *ACS Appl Mater Interfaces* 10:26274–26282
29. Zhou T, Lv W, Li J, Zhou G, Zhao Y, Fan S, Liu B, Li B, Kang F, Yang Q-H (2017) Twinborn  $TiO_2$ - $TiN$  heterostructures enabling smooth trapping-diffusion-conversion of polysulfides towards ultralong life lithium-sulfur batteries. *Energy Environ Sci* 10:1694–1703
30. Xu J, Tang W, Yang C, Manke I, Chen N, Lai F, Xu T, An S, Liu H, Zhang Z, Cao Y, Wang N, Zhao S, Niu D, Chen R (2021) A highly conductive COF@CNT electrocatalyst boosting polysulfide conversion for Li-S chemistry. *ACS Energy Lett* 6:3053–3062
31. Zhao CX, Li XY, Zhao M, Chen ZX, Song YW, Chen WJ, Liu JN, Wang B, Zhang XQ, Chen CM, Li BQ, Huang JQ, Zhang Q, Molecular SI (2021) Electrocatalysts for high-performance lithium-sulfur batteries. *J Am Chem Soc* 143:19865–19872
32. Zhang K, Liu W, Gao Y, Wang X, Chen Z, Ning R, Yu W, Li R, Li L, Li X, Yuan K, Ma L, Li N, Shen C, Huang W, Xie K, Loh KP (2020) A High-performance lithium metal battery with ion-selective nanofluidic transport in a conjugated microporous polymer protective layer. *Adv Mater* 33:2006323
33. Yang Y, Meng G, Wang H, Wang W, Zhang J (2023) Efficient polysulfides trapping and redox enabled by Co/N-carbon implanted  $Li^+$ -montmorillonite for advanced lithium-sulfur batteries. *Chem Eng J* 45:1138914
34. Lan Y, Liu Y, Li J, Chen D, He G, Parkin IP (2021) Natural clay-based materials for energy storage and conversion applications. *Adv Sci*. <https://doi.org/10.1002/advs.202004036>
35. Zeng Z, Dong Y, Yuan S, Zhao W, Wang L, Liu S, Yang Y, Ge P, Sun W, Ji X (2022) Natural mineral compounds in energy-storage systems: development, challenges, prospects. *Energy Storage Mater* 45:442–464
36. Tu S, Chen X, Zhao X, Cheng M, Xiong P, He Y, Zhang Q, Xu Y (2018) A polysulfide-immobilizing polymer retards the shuttling of polysulfide intermediates in lithium-sulfur batteries. *Adv Mater* 30(45):1804581
37. Yoo J, Cho SJ, Jung GY, Kim SH, Choi KH, Kim JH, Lee CK, Kwak SK, Lee SY (2016) COF-Net on CNT-Net as a molecularly designed, hierarchical porous chemical trap for polysulfides in lithium-sulfur batteries. *Nano Lett* 16:3292–3300
38. Li Y, Yu J (2021) Emerging applications of zeolites in catalysis, separation and host-guest assembly. *Nat Rev Mater* 6:1156–1174
39. Maiti S, Sclar H, Wu X, Grinblat J, Talianker M, Kondrakov A, Markovsky B, Aurbach D (2023) Zeolites as multifunctional additives stabilize high-voltage Li-batteries based on  $LiNi_0.5Mn_1.5O_4$  cathodes, mechanistic studies. *Energy Storage Mater* 56:25–39
40. Liu F, Cui Y (2021) Zeolite-based electrolyte accelerating the realization of solid-state li-air battery. *Chem Res Chin Univ* 37:801–802
41. Barbosa JC, Gonçalves R, Costa CM, de Zea Bermudez V, Fidalgo-Marijuan A, Zhang Q, Lanceros-Méndez S (2021) Metal-organic frameworks and zeolite materials as active fillers for lithium-ion battery solid polymer electrolytes. *Mater Adv* 2:3790–3805
42. Ding Z, Tang Q, Zhang Q, Yao P, Liu X, Wu J (2023) A flexible solid polymer electrolyte enabled with lithiated zeolite for high performance lithium battery. *Nano Res* 16:9443–9452
43. Chi X, Li M, Di J, Bai P, Song L, Wang X, Li F, Liang S, Xu J, Yu J (2021) A highly stable and flexible zeolite electrolyte solid-state Li-air battery. *Nature* 592(7855):551–557
44. Bai S, Liu X, Zhu K, Wu S, Zhou H (2016) Metal-organic framework-based separator for lithium-sulfur batteries. *Nat Energy* 1:16094
45. Yang Y, Mu P, Li B, Li A, Zhang J (2022) In situ separator modification with an N-rich conjugated microporous polymer for the effective suppression of polysulfide shuttle and Li dendrite growth. *ACS Appl Mater Interfaces* 14:49224–49232

46. Yang Y, Zhang J (2018) Highly stable lithium-sulfur batteries based on laponite nanosheet-coated celgard separators. *Adv Energy Mater* 8:1801778
47. Wang Y, Wu Y, Mao P, Fan Y, Wang X, Xiang H, Li Z, Li K, Hu C (2024) A kegglin Al13-montmorillonite modified separator retards the polysulfide shuttling and accelerates Li-ion transfer in Li-S batteries. *Small* 20(1):2304898
48. Abbas S, Ding J, Wu S, Fang J, Orcid K, Mohapatra A, Lee L, Wang P, Chang C, Chu C (2017) Modified separator performing dual physical/chemical roles to inhibit polysulfide shuttle resulting in ultrastable Li-S batteries. *ACS Nano* 11:12436–12445
49. Liu R, Wei Z, Peng L, Zhang L, Zohar A, Schoeppner R, Wang P, Wan C, Zhu D, Liu H, Wang Z, Tolbert SH, Dunn B, Huang Y, Sautet P, Duan X (2024) Establishing reaction networks in the 16-electron sulfur reduction reaction. *Nature* 626:98–104
50. Wang L, Wang T, Peng L, Wang Y, Zhang M, Zhou J, Chen M, Cao J, Fei H, Duan X, Zhu J (2022) The promises, challenges and pathways to room-temperature sodium-sulfur batteries. *Nat Sci Rev.* <https://doi.org/10.1093/nsr/nwab050>
51. Yim T, Han SH, Park NH, Park M-S, Lee JH, Shin J, Choi JW, Jung Y, Jo YN, Yu JS, Kim KJ (2016) Effective polysulfide rejection by dipole-aligned BaTiO<sub>3</sub> coated separator in lithium-sulfur batteries. *Adv Func Mater* 26:7817–7823
52. Zang Y, Pei F, Huang J, Fu Z, Xu G, Fang X (2018) Large-area preparation of crack-free crystalline microporous conductive membrane to upgrade high energy lithium-sulfur batteries. *Adv Energy Mater* 8:1802052

**Publisher's Note** Springer Nature remains neutral with regard to jurisdictional claims in published maps and institutional affiliations.

Springer Nature or its licensor (e.g. a society or other partner) holds exclusive rights to this article under a publishing agreement with the author(s) or other rightsholder(s); author self-archiving of the accepted manuscript version of this article is solely governed by the terms of such publishing agreement and applicable law.

## Authors and Affiliations

Huajin Mao<sup>1</sup> · Lijuan Yi<sup>2</sup> · Wanning Li<sup>3</sup>

✉ Huajin Mao  
maohuajincw@163.com

<sup>1</sup> College of Architecture and Surveying Engineering,  
Shanxi Datong University, Datong 037003,  
People's Republic of China

<sup>2</sup> Datong Vocational and Technical College of Coal,  
Datong 037003, People's Republic of China

<sup>3</sup> Henan Water Planning, Design and Research Co., Ltd.,  
Anyang 455000, People's Republic of China